Critical Size and Nucleation Field of Ideal Ferromagnetic Particles*

E. H. FREI, S. SHTRIKMAN, AND D. TREVES
Department of Electronics, the Weizmann Institute of Science, Rehovoth, Israel
(Received November 14, 1956; expanded manuscript received January 23, 1957)

The field at which the spins of a previously saturated ideal ferromagnetic particle cease to be aligned is defined as the nucleation field. This field is calculated, using calculus of variation, for an infinite cylinder and a sphere, assuming three mechanisms of magnetization reversal: spin rotation in unison, magnetization curling, and magnetization buckling. Theoretical treatment shows that, in fact, only curling and rotation in unison need be considered.

The critical size for single-domain behavior, defined as the largest size at which magnetization reversal proceeds by rotation in unison, is calculated for the prolate ellipsoid and is found to be practically independent of magnetocrystalline anisotropy and elongation and approximately equal to $A^{\frac{1}{2}}/I_s$. Here A is the exchange constant and I_s is the saturation magnetization.

For cylinders larger than the critical size, the coercive force, for a field applied in the direction of the long axis, is found to be equal to the nucleation field, when magnetocrystalline anisotropy is neglected. The coercive force thus calculated decreases with the radius of the cylinder, R, according to $H_c=6.78A/I_sR^2$.

Available experimental data are discussed and are generally found to be in a better agreement with this than with previous theory.

1. INTRODUCTION

IN the last decade, interest in powder magnets has increased appreciably. In particular the high-energy products promised by current theory[1-6] for elongated iron fine-particle magnets promoted investigation in this field. This theory suggests that the magnetization changes in particles below a certain size (the critical size) occur by spin rotation in unison.[1,7,8] The particles are assumed to be always saturated and are referred to as "single-domain particles." The coercive force depends on the various magnetic anisotropies,[1,9] and thus is generally calculated to be quite high.

The critical size is calculated by comparing the energy of the single-domain configuration with the energy of configurations which tend towards flux closure. The calculation is carried out for zero external field. Figure 1 shows the flux closure arrangement (ring model) usually assumed for prolate ellipsoids which are thin compared to the wall thickness.[8,10] The critical size in this case, as derived in Appendix I, is given by

$$N_bI_s^2R_c^2/6A=\ln(4R_c/a)-1, \qquad (1)$$

where I_s is the saturation magnetization, R_c—the critical radius, a—the lattice constant, N_b—the demagnetizing coefficient along the polar axis,[11] and A—the exchange constant[12] (which is also referred to as the stiffness constant,[13] or the Bloch wall coefficient[14]). From (1) it is seen that for $N_b\to 0$ (an infinite cylinder), $R_c\to\infty$, since the self magnetostatic energy is zero.

In the current theory there are three points the validity of which must be questioned.

(1) The calculation is carried out by tacitly assuming that if the particle is a single domain at zero field, it will stay saturated under any field. This means that the changes of magnetization occur by rotation in unison. It will be shown that this assumption is not valid for many cases and leads to erroneous conclusions concerning the coercive force.[15]

(2) The second point to be questioned is the stability of the states compared in order to calculate the critical size. Any static physical state should be of minimum free energy (not necessarily an absolute minimum). It is shown in Appendix II that some of the configurations discussed do not obey this criterion. Although the states discussed are usually a good approximation to the minimum energy states, yet, in some cases, as in the evaluation of the remanence, they lead to erroneous conclusions.

(3) The method of comparing the energy of different configurations in order to find the actual state of magnetization should be questioned as it does not allow for the existence of hysteresis which is of fundamental importance in ferromagnetism. It is easy to see that if this method is followed consistently, the coercive force vanishes identically as all magnetic energies concerned are invariant to inversion of the magnetization except the energy of interaction with the external field which changes its sign.

* This paper represents part of a thesis to be submitted by one of the authors (S.S.) to the Israel Institute of Technology (TECHNION), in partial fulfilment of the requirements for the D.Sc. degree.

[1] E. C. Stoner and E. P. Wohlfarth, Trans. Roy. Soc. (London) **A240**, 599 (1948).
[2] Mendelson, Luborsky, and Paine, J. Appl. Phys. **26**, 1274 (1955).
[3] Paine, Mendelson, and Luborsky, Phys. Rev. **100**, 1055 (1955).
[4] I. S. Jacobs and C. P. Bean, Phys. Rev. **100**, 1060 (1955).
[5] E. H. Carman, Brit. J. Appl. Phys. **6**, 426 (1955).
[6] Session on Permanent Magnets and Fine Particles, *Proceedings of the Boston Conference on Magnetism and Magnetic Materials* (to be published).
[7] C. Kittel, Phys. Rev. **70**, 965 (1946).
[8] L. Néel, Compt. rend. **224**, 1488, 1550 (1947).
[9] C. Kittel, Revs. Modern Phys. **21**, 544 (1949).
[10] A. H. Morrish and S. P. Yu, J. Appl. Phys. **26**, 1049 (1955).
[11] E. C. Stoner, Phil. Mag. **36**, 803 (1945).
[12] C. Kittel, Revs. Modern Phys. **21**, 552 (1949).
[13] E. P. Wohlfarth, Proc. Phys. Soc. (London) **A65**, 1053 (1952).
[14] C. Herring, Phys. Rev. **85**, 1003 (1952).
[15] S. Shtrikman and D. Treves, Bull. Research Council Israel (to be published).

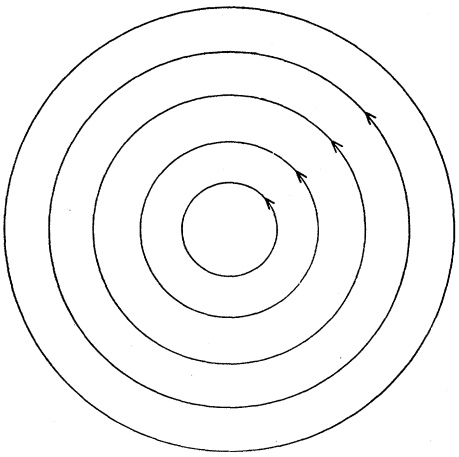

FIG. 1. Illustration of flux closure produced by a ring configuration in the equatorial plane of the prolate ellipsoidal particle.

In the following the behavior of ferromagnetic particles is analyzed avoiding the arbitrary assumptions discussed above. The calculations are based on the following model:

(1) The particle discussed is a single-crystal prolate ellipsoid, having no imperfections.

(2) The energies taken into account are E_K, the magnetocrystalline energy, E_m, the self-magnetostatic energy, E_x, the exchange energy, and E_H, the energy of interaction with the external field. All other energies are neglected.

(3) The exchange energy is represented by[12]

$$E_x = A \sum_i (\nabla \alpha_i)^2, \tag{2}$$

where α_i are the direction cosines of the magnetization vector, assumed to be continuous differentiable functions of the coordinates.

(4) No distinction is made between total energy and free energy, assuming the analysis to be valid only for temperatures far below the Curie temperature.

(5) The analysis assumes static ferromagnetism.[16] All effects associated with the time rate of change of magnetization are not considered.

The magnetic state of the particle is completely described by the direction cosines α_i of the magnetization at every point, and these are found by minimizing the total energy E. The calculation will be best explained by going through some examples in detail. The magnetic behavior of the infinite cylinder is analyzed in paragraph 2. This is done by studying three different modes of magnetization change. The dependence of the coercive force of the infinite cylinder on its radius is found. The behavior of the sphere and the prolate ellipsoid are studied in paragraphs 3 and 4 respectively and the critical size for single-domain behavior is evaluated.

[16] J. L. Snoek, *New Developments in Ferromagnetic Materials* (Elsevier Publishing Company, Amsterdam, 1947), Chap. 1.

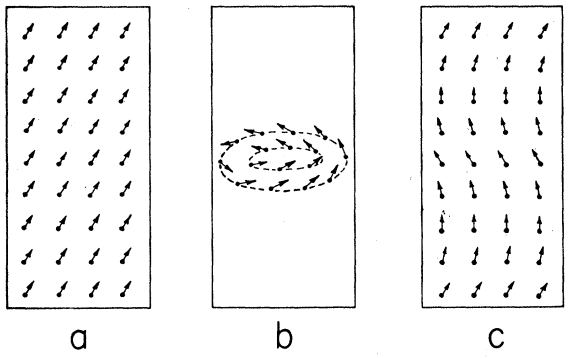

FIG. 2. Modes of magnetization change for the infinite cylinder: (a) spin rotation in unison; (b) magnetization curling; (c) magnetization buckling.

2. THE INFINITE CYLINDER

Let an infinite cylinder of radius R be defined in a cylindrical coordinate system (r,φ,z). Let the z axis coincide with the direction of the external field. If this field is strong enough, there is only one state of stable equilibrium; namely, all spins aligned in the direction of the field. (Crystal anisotropy E_K is neglected for the time being.) Decreasing the field, a negative value is reached for which this state ceases to be a minimum energy state. To find the field dependence of the magnetization state, one should find the direction cosine functions, $\alpha_i(r,\varphi,z)$, that minimize the total energy. This is a rather complicated variational problem. To facilitate the calculation a bit of guesswork is done, guided by symmetry considerations and making use of known low-energy configurations. Along these lines, three ways of magnetization change, as illustrated in Fig. 2, are considered:

(1) spin rotation in unison;
(2) magnetization curling;
(3) magnetization buckling.

A. Spin Rotation in Unison

This case has already been discussed in detail.[1,9] The hysteresis loop is rectangular, and the coercive force is

$$h_c = 1 \tag{3}$$

in terms of the reduced field

$$h = H/2\pi I_s. \tag{4}$$

B. Magnetization Curling

In this case the magnetization changes occur by spin rotation from the z axis in a plane perpendicular to the radius. The angle ω between the spin direction and the z axis is independent of φ and z, and thus a function of r alone. The total energy E consists of E_x and E_H

only, since in this case $E_m=0$,

$$\bar{E}=\frac{1}{\pi R^2}\int_{a/2}^{R}(E_x+E_H)2\pi r dr, \tag{5}$$

where $\bar{E}$ is the mean total energy per unit volume and a is the lattice constant. Following Néel[8] the lower limit of integration is taken as $a/2$.

Substituting the direction cosines,

$$\alpha_x=\sin\omega\cos\varphi,\quad \alpha_y=\sin\omega\sin\varphi,\quad \alpha_z=\cos\omega, \tag{6}$$

in Eq. (2), one gets

$$E_x=A[(d\omega/dr)^2+(1/r^2)\sin^2\omega]. \tag{7}$$

The energy of interaction with the external field is given by

$$E_H=-HI_s\cos\omega. \tag{8}$$

Using (4) and substituting

$$x=r/R,\quad R_0=A^{\frac{1}{2}}/I_s,\quad S=R/R_0 \tag{9}$$

in (5), one obtains

$$\bar{E}=\frac{2A}{R^2}\int_{a/2R}^{1}\left[x\left(\frac{d\omega}{dx}\right)^2+\frac{\sin^2\omega}{x}-2\pi S^2hx\cos\omega\right]dx. \tag{10}$$

The Euler differential equation[17] which minimizes the integral (10) is

$$\frac{d^2\omega}{dx^2}+\frac{1}{x}\frac{d\omega}{dx}-\left(h\pi S^2+\frac{\cos\omega}{x^2}\right)\sin\omega=0, \tag{11}$$

with the boundary conditions for mobile limits[18]:

$$d\omega/dx=0,\quad \text{for}\quad x=a/2R\quad\text{and}\quad x=1. \tag{12}$$

The trivial solution $\omega=0$ is readily verified to be valid for any value of h. However, this solution is a minimum only for a certain range of h. The value of h where $\omega=0$ stops being a minimum is defined as the reduced nucleation field h_n.

In order to find h_n, only small angles need be considered, i.e.,

$$\omega\ll 1. \tag{13}$$

This simplification linearizes the differential equation (11) to the Bessel equation

$$d^2\omega/dx^2+x^{-1}d\omega/dx-(h\pi S^2+x^{-2})\omega=0, \tag{14}$$

the solution of which is

$$\omega=BJ_1[(-h\pi)^{\frac{1}{2}}Sx]+CN_1[(-h\pi)^{\frac{1}{2}}Sx]. \tag{15}$$

Here B and C are constants, and J_1 and N_1 are the Bessel and Neumann functions of the first order, respectively.

[17] H. Margenau and G. M. Murphy, *The Mathematics of Physics and Chemistry* (D. Van Nostrand Company, Inc., New York, 1956), second edition, pp. 198–200.

[18] See reference 17, pp. 214 and 215.

If $a/2R\ll 1$, a good approximation is obtained assuming $\omega=0$ for $x=0$, so that one obtains $C=0$. (The exact solution is given in Appendix III.) The boundary condition for $x=1$ is

$$B\frac{d}{dx}J_1[(-h\pi)^{\frac{1}{2}}Sx]=0, \tag{16}$$

so that either $B=0$ or

$$\left\{\frac{d}{dx}J_1[(-h\pi)^{\frac{1}{2}}Sx]\right\}_{x=1}=0. \tag{17}$$

When $h=h_i$ is such that Eq. (17) is fulfilled, the second variation of E at $\omega=0$ vanishes. The smallest h_i will accordingly be the nucleation field. Now the first maximum[19] of $J_1(y)$ is given by

$$y=1.841, \tag{18}$$

so that

$$h_n=1.08S^{-2}. \tag{19}$$

In Appendix IV it is shown that at the nucleation field, ω, changes discontinously. A graphical solution of (11) and an approximate solution using the Ritz method[20] suggest that the magnetization reverses completely, coming to the second trivial solution of (11), $\omega=\pi$.

This means that here again the hysteresis loop is rectangular with $h_n=h_c$.

C. Magnetization Buckling

In this case spin rotation occurs in the x direction alone. The spin deviation is a periodic function of z, having a period of $2T$. In order to calculate the nucleation field which will generally be defined as the field at which the spins cease to be aligned, let the angle ω between the spins direction and the z axis be given by the Fourier expansion

$$\omega=\sum_{m=1}^{\infty}\omega_{2m-1}\cos\left[(2m-1)\frac{\pi}{T}z\right]. \tag{20}$$

Substituting the direction cosines

$$\alpha_x=\sin\omega,\quad \alpha_y=0,\quad \alpha_z=\cos\omega,$$

into Eq. (2), and using (20), one gets

$$\bar{E}_x=A\sum_{m=1}^{\infty}\tfrac{1}{2}\omega_{2m-1}^2(2m-1)^2(\pi/T)^2. \tag{21}$$

To evaluate the self-magnetostatic energy, the surface and the volume charges are considered. However, the surface charges are proportional to ω while the volume charges are proportional to ω^2 and can thus be neglected

[19] G. Petieu, *La Théorie des Fonctions de Bessel* (Centre National de la Recherche Scientifique, Paris, 1955), p. 452.

[20] See reference 17, p. 377.

in the evaluation of the nucleation. The surface charges σ are given by

$$\sigma = I_s \cos\varphi \sin\omega. \tag{22}$$

Since $\omega \ll 1$ is assumed, one obtains, using (20),

$$\sigma = I_s \cos\varphi \sum_{m=1}^{\infty} \omega_{2m-1} \cos\left[(2m-1)\frac{\pi}{T}z\right]. \tag{23}$$

The energy associated with the surface charges is evaluated in Appendix V and is given by

$$\bar{E}_m = \tfrac{1}{2}\sum_{m=1}^{\infty} \omega_{2m-1}{}^2 \pi^2 I_s{}^2 i J_1\left[i(2m-1)\frac{\pi}{T}R\right] \times H_1{}^{(1)}\left[i(2m-1)\frac{\pi}{T}R\right]. \tag{24}$$

Using (8) and (20), one finds

$$\bar{E}_H = \frac{HI_s}{4}\sum_{m=1}^{\infty} \omega_{2m-1}{}^2. \tag{25}$$

Using (4), (23), (24), (25) and writing $\pi R/T = L$, the total energy is

$$\bar{E} = \frac{\pi}{2} I_s{}^2 \sum_{m=1}^{\infty} \omega_{2m-1}{}^2 \left\{ \frac{L^2(2m-1)^2}{\pi S^2} + \pi i J_1[i(2m-1)L] H_1{}^{(1)}[i(2m-1)L] + h \right\}. \tag{26}$$

A necessary condition for nucleation is that the Hessian[21] $|\mathfrak{H}|$ of $\bar{E}$ with respect to the variables ω_{2m-1} is zero. This implies that

$$|\mathfrak{H}| \equiv \left| \frac{\partial^2 E}{\partial\omega_i \partial\omega_k} \right| = 0. \tag{27}$$

Since in this case $\mathfrak{H}$ is diagonalized, (27) becomes

$$\prod_{m=1}^{\infty} \frac{\partial^2 E}{\partial \omega_{2m-1}{}^2} = 0. \tag{28}$$

The lowest value of h satisfying (28) or explicitly

$$h + \frac{L^2(2m-1)^2}{\pi S^2} + \pi i J_1[i(2m-1)L] H_1{}^{(1)}[i(2m-1)L] = 0 \tag{29}$$

is the nucleation field.

Since h is a function of $L(2m-1)$ only, $m=1$ is chosen for simplicity. Minimizing h with respect to iL yields

$$\frac{2L}{\pi S^2} = \pi \frac{d}{d(iL)}[J_1(iL) H_1{}^{(1)}(iL)]. \tag{30}$$

[21] A. C. Aitken, *Determinants and Matrices* (Oliver and Boyd, Edinburgh and London, 1949), sixth edition, pp. 130–131.

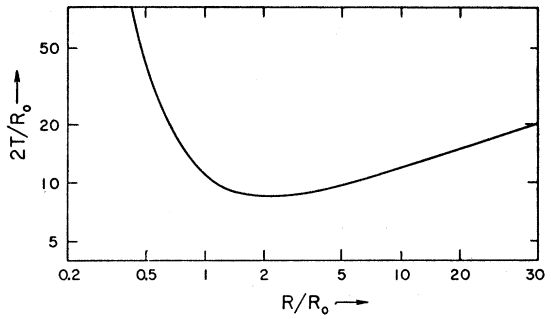

FIG. 3. Theoretical plot of the nucleation wavelength $2T$ for the buckling mechanism in an infinite cylinder *versus* its radius R. $R_0 = A^{\frac{1}{2}}/I_s$ is the characteristic radius of the material, A is the exchange constant, and I_s is the saturation magnetization.

From Eq. (30) the nucleation wave number $L_n(S)$ is calculated. By substituting it in (29), $h_n(S)$ is obtained. Figure 3 shows $2T/R_0 = f(S)$.

For $L_n \to 0$, $h_n \to 1$. This is found by using[22]

$$\lim_{x\to 0} i J_1(ix) H_1{}^{(1)}(ix) = 1/\pi. \tag{31}$$

The solution of (30) gives in this case $S \to 0$. This means that only in the limiting case $R=0$, does the buckling mechanism degenerate into rotation in unison.

For $S \to \infty$, $L \to \infty$, and using[23]

$$\lim_{L\to\infty} i J_1(iL) H_1{}^{(1)}(iL) = 1/\pi L \tag{32}$$

and Eq. (30), the asymptotic relation for $S \to \infty$ is found to be

$$L_n = (\tfrac{1}{2}\pi S^2)^{\frac{1}{3}} = 1.16 S^{\frac{2}{3}}. \tag{33}$$

From (29), one calculates that, for large values of S,

$$h_n = -3/2L_n = -(3/2)(2/\pi)^{\frac{1}{3}} S^{-\frac{2}{3}} = -1.29 S^{-\frac{2}{3}}. \tag{34}$$

In the intermediate region, Eqs. (29) and (30) are solved numerically with the help of the relations:

$$\begin{aligned} dJ_1(x)/dx &= J_0(x) - J_1(x)/x, \\ dH_1{}^{(1)}(x)/dx &= H_0{}^{(1)}(x) - H^{(1)}(x)/x, \end{aligned} \tag{35}$$

and tabulated Bessel functions.[24]

It is obvious that of the three mechanisms discussed, the physical system will choose the one yielding the most positive h_n. The results of the calculations are plotted in Fig. 4. It is seen that for $S > 1.1$, the curling takes place and for $S < 1.1$, buckling is the acting mechanism while rotation in unison is equivalent to buckling for $S \ll 1$.

It is believed that the transition from buckling to curling is not abrupt, and that in the neighborhood of $S=1$, a mixed mechanism takes place somewhat lowering the value of $|h_n|$ in that region. It should be noted

[22] See reference 17, p. 113 and p. 120.
[23] See reference 17, p. 119.
[24] E. Jahnke and F. Emde, *Tables of Functions* (Dover Publications, New York, 1945), fourth edition, pp. 226–243.

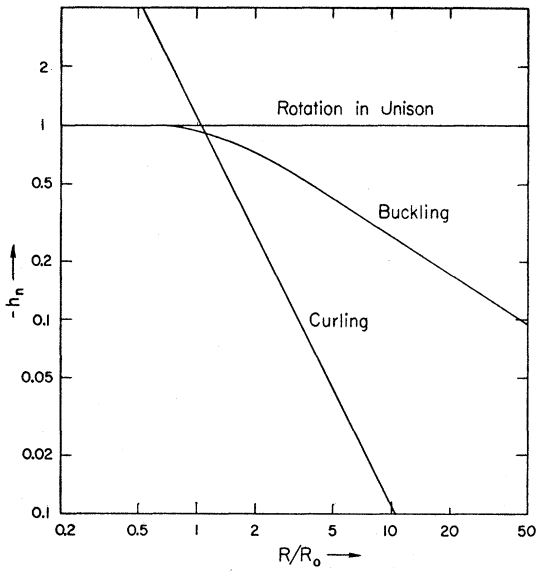

FIG. 4. Theoretical plot of the nucleation field of an infinite cylinder *versus* its radius R for magnetization curling and magnetization buckling. The field is applied along the axis of the cylinder. The nucleation field H_n is given by $2\pi I_s h_n$, where I_s is the saturation magnetization. $R_0=A^{\frac{1}{2}}/I_s$ is the characteristic length of the material, and A is the exchange constant. The coercive force for rotation in unison is given for comparison.

that although not rigorously proved, it is believed that the hysteresis loop for the cylinder whose axis is parallel to the applied field, is always rectangular, thus identifying the nucleation field with the coercive force.

3. THE SPHERE

The nucleation field for the sphere is calculated under the assumption of the curling mechanism. The spherical coordinate system (r,φ,θ) is introduced. The direction of the external field is assumed to coincide with $\theta=0$. In the following calculations the angle ω, as previously defined, depends on r and θ only. When one substitutes (6) in (2) and writes the gradient in spherical coordinates, the exchange energy becomes

$$E_x=A[(\partial\omega/\partial r)^2+r^{-2}(\partial\omega/\partial\theta)^2+\sin^2\omega/(r^2\sin^2\theta)]. \quad (36)$$

For this mechanism, when $\omega\ll 1$, the self-magnetostatic energy can be approximated by

$$E_m=\tfrac{2}{3}\pi I_s^2-\tfrac{4}{3}\pi I_s^2\omega^2/2. \quad (37)$$

The variable part of the total energy, if one neglects terms in powers higher than ω^2 and assumes $E_K=0$, is given by

$$\bar{E}=\tfrac{3}{2}R^{-3}\int_0^\pi\int_0^R\{A[(\partial\omega/\partial r)^2+(1/r^2)(\partial\omega/\partial\theta)^2+\omega^2/(r^2\sin^2\theta)]-(4\pi I_s/3-H)I_s^2/2\}r^2dr\sin\theta d\theta. \quad (38)$$

The choice of the lower limit of r is thought to be a good approximation in view of the results obtained in Appendix III. When one uses (9), the energy becomes

$$\bar{E}=\frac{3A}{2R^2}\int_0^\pi\int_0^1[(\partial\omega/\partial x)^2+(1/x^2)(\partial\omega/\partial\theta)^2+\omega^2/(x^2\sin^2\theta)-(h-\tfrac{2}{3})\pi S^2]x^2dx\sin\theta d\theta. \quad (39)$$

The Euler equation[25] is

$$\partial^2\omega/\partial x^2+(2/x)\partial\omega/\partial x+(1/x^2)\partial^2\omega/\partial\theta^2+(1/x^2)\cot\theta(\partial\omega/\partial\theta)-[(h-\tfrac{2}{3})\pi S^2+1/(x^2\sin^2\theta)]\omega=0, \quad (40)$$

with the boundary conditions[26]

$$(\partial\omega/\partial x)_{x=1}=0 \quad \text{and} \quad \omega=0, \quad \text{on the} \quad \theta=0 \text{ axis.} \quad (41)$$

Equation (40) is solved by separation of variables. Substituting $\omega=\Theta(\theta)X(x)$, one gets the two differential equations

$$d^2X/dx^2+(2/x)dX/dx-[(h-\tfrac{2}{3})\pi S^2+b(b+1)/x^2]X=0, \quad (42)$$

$$d^2\Theta/d\theta^2+\cot\theta d\Theta/d\theta-[1/\sin^2\theta-b(b+1)]\Theta=0, \quad (43)$$

where b is an integer. The solution of these equations[27] leads to

$$\omega=\textstyle\sum_b C_b P_b^1(\cos\theta)x^{-\frac{1}{2}}J_{b+\frac{1}{2}}\{Sx[-\pi(h-\frac{2}{3})]^{\frac{1}{2}}\},$$

where C_b are constants, P_b^1 are Legendre's associated functions of the first kind, and $J_{b+\frac{1}{2}}$ are Bessel functions of half odd order. The condition at $\theta=0$ is identically fulfilled. However, in order that ω remains finite for $x=0$, one needs $b>0$. The lowest h fulfilling the second boundary condition,

$$d\{x^{-\frac{1}{2}}J_{b+\frac{1}{2}}[Sx(-\pi(h-\tfrac{2}{3}))^{\frac{1}{2}}]\}/dx=0 \quad \text{for} \quad x=1, \quad (44)$$

is h_n and is given for $b=1$.

Substituting the relation[28]

$$(\pi y/2)^{\frac{1}{2}}J_{\frac{3}{2}}(y)=\sin y/y-\cos y \quad (45)$$

in (44), one gets

$$2y\cot y-2+y^2=0, \quad (46)$$

where

$$y=S[-\pi(h-\tfrac{2}{3})]^{\frac{1}{2}}. \quad (47)$$

The smallest solution of (46) is

$$y^2=4.35,$$

and using this value one obtains from (47)

$$h_n=\tfrac{2}{3}-1.39S^{-2}. \quad (48)$$

Equation (48) is valid only for positive values of h_n. Negative values of h_n have no physical significance as the coercive force for spin rotation in unison is zero in

[25] See reference 17, pp. 207 and 208.
[26] A. R. Forsyth, *Calculus of Variations* (Cambridge University Press, Cambridge, 1927), p. 468.
[27] See reference 17, pp. 234 and 235.
[28] See reference 17, p. 118.

this case. (It should be noted that also for positive h_n the coercive force is zero, as crystalline anisotropy was neglected here.) This immediately yields the critical size for single-domain behavior:

$$S_c=1.44.$$

4. THE PROLATE ELLIPSOID

The first term in the right-hand side of Eq. (48) comes from the demagnetizing field. Analogously the nucleation field for the prolate ellipsoid with the external field along the polar axis is

$$h_n=N_b/2\pi-kS^{-2}. \tag{49}$$

Here k is a constant which varies from 1.08 for the cylinder to 1.39 for the sphere.

From Fig. 4 it is seen that a good approximation to the behavior of the cylinder can be made by neglecting the buckling mechanism and taking the rotation in unison instead.

If the coercive force h_c for rotation in unison[1] as given by

$$h_c=(N_b-N_a)/2\pi \tag{50}$$

is larger than h_n as defined in (49), rotation in unison takes place, and the particle will behave as a single domain. Here N_b and N_a are the demagnetizing factors along the polar axis and an axis perpendicular to it, respectively. Equating (49) and (50) gives the critical size,

$$S_c^2=2\pi k/N_a. \tag{51}$$

From the variation of N_a and k, one finds that

$$1.04\leqslant S_c\leqslant 1.44. \tag{52}$$

The higher value of S_c is for the sphere and the lower for the cylinder. This result shows that contrary to current belief, the critical size for single-domain behavior is practically independent of elongation, and is approximately equal to R_0. When anisotropy is taken into account, with the easy direction of magnetization coinciding with the polar axis, an equal term $K/\pi I_s^2$ will be added to both h_n and h_c, so that the critical radius will not be affected.

The fact that the critical size is independent of magnetocrystalline anisotropy can be best understood from the nature of the energies concerned. The exchange energy tends to keep the spins aligned while the self magnetostatic energy tends to minimize the free charges by forcing flux closure paths. On the other hand, the magnetocrystalline energy is a local effect and thus is independent of the form of nucleation. The exchange energy is caused by short-range forces and is predominant for small sizes, causing the single-domain behavior. The magnetostatic energy, being a long-range effect, predominates for large sizes, causing magnetization changes to occur by flux closure mechanisms and thus not allowing rotation in unison.

These speculations show that the critical size is a function of I_s and A only. Following this idea, dimensional analysis shows that the critical size must be proportional[29] to $A^{\frac{1}{2}}/I_s$ which equals R_0, the characteristic length of the material.

In this paper, only the nucleation field was calculated for the prolate ellipsoid. Brown[30] had already pointed out in 1940 the way to find the exact hysteresis curve of an ideal ferromagnetic particle, by solving a set of nonlinear partial differential equations. However, this is a formidable problem and is not easily tackled.

5. DISCUSSION

The results of the above calculation show that below a certain size (the critical size) the ferromagnetic particle behaves approximately as a single domain. It is found, contrary to current belief, that the critical size is independent of crystal anisotropy and is almost independent of elongation.

It follows from previous theory that an abrupt decrease in the coercive force at the critical size should occur from the relatively high value given by the magnetic anisotropy to the low value associated with domain wall movements. Bertaut,[31] Carman,[5] and Meiklejohn[32] found experimentally that the coercive force of iron powders is inversely proportional to the particle size. Similar behavior was reported by Néel[33] as having been found by Gottshalk for magnetite powder. The calculations given in this paper suggest a gradual decrease of the coercive force with particle size in cases where shape anisotropy predominates.

The absolute value of the coercive force obtained experimentally for supposedly single-domain powders is usually considerably less than that predicted by the previous theory.[2,3,10,32] Furthermore, Morrish and Yu[34] remarked that there is in fact some evidence that the coercive force continues to increase for particles smaller than the supposed critical size. When one compares the conclusions of this paper with experiments, difficulties[35] are encountered in determining the value of A needed to calculate R_0. Even for iron, which is the material most studied, the value suggested for A varies considerably, starting from $A=0.3\times10^{-6}$ erg/cm (as given by Wohlfarth[13]) through 0.83×10^{-6} (Stoner[35]), 1.16×10^{-6} (Néel[8]), to 2×10^{-6} (Kittel[12]). Choosing $A=10^{-6}$ with $I_s=1700$ gauss, one finds from (9) that $R_0=60$ A. For magnetite, choosing $A=10^{-6}$ erg/cm following Galt,[36] and $I_s=500$, one finds $R_0\approx200$ A. One sees that the critical size, which is approximately

[29] After completion of this work, it came to our notice that Dr. W. F. Brown reported a similar result at the Thanksgiving meeting of the American Physical Society, 1956 [W. F. Brown, Bull. Am. Phys. Soc. Ser. II, 1, 323 (1956)].

[30] W. F. Brown, Phys. Rev. **58**, 736 (1940).

[31] F. Bertaut, Compt. rend. **229**, 417 (1949).

[32] W. Meiklejohn, Revs. Modern Phys. **25**, 302 (1953).

[33] L. Néel, *Advances in Physics* (Taylor and Francis, Ltd., London, 1955), Vol. 4, p. 191.

[34] S. P. Yu and A. H. Morrish, Phys. Rev. **102**, 670 (1956).

[35] E. C. Stoner, Repts. Progr. in Phys. **13**, 111 (1950).

[36] J. K. Galt, Phys. Rev. **85**, 664 (1952).

equal to R_0, is smaller than that expected by current theory.[8,10] These rather low values of the critical size suggest that the above-mentioned effects might be explained by the fact that the critical size was not reached in these experiments.

One must also admit the possibility that upon decreasing the size the particles will become paramagnetic[37] before reaching the size of single-domain behavior.

In cases where $K \gg I_s^2$, as in MnBi and Ferroxdure, the theory disagrees completely with experiment[38] since, according to theory, the coercive force is independent of particle size. This was already pointed out by Brown.[39] Thus the model assumed does not apply in this case. It is possible that a model taking into account imperfections, might help in solving this discrepancy.[40]

ACKNOWLEDGMENTS

The authors wish to thank A. Aharoni, H. Jarosch, and Dr. J. Kaplan for valuable discussions.

APPENDIX I. CALCULATION OF THE CRITICAL SIZE OF THE PROLATE ELLIPSOID ACCORDING TO THE RING MODEL

The critical size for this model is calculated by comparing the magnetostatic energy to the exchange energy. Taking $\omega=\pi/2$ in (7), one finds for the exchange energy density

$$E_x = A/r^2. \tag{53}$$

When one uses (53), the exchange energy $\bar{E}_x$ of the ellipsoid per unit volume is

$$(4/3)\pi R^2 b \bar{E}_x = \int_{a/2}^{R}\int_{0}^{b[1-(r/R)^2]^{\frac{1}{2}}} 2\pi r^{-1} dz dr = 4\pi A b[\ln(4R/a)-1], \tag{54}$$

where $2R$ and $2b$ are the short axis and the long axis of the ellipsoid, respectively.

The magnetostatic energy is

$$\bar{E}_m = \tfrac{1}{2} N_b I_s^2, \tag{55}$$

where N_b is the demagnetizing coefficient along the polar axis. Comparison of (54) and (55) yields the critical size R_c:

$$(N_b/6A) I_s^2 R_c^2 = \ln(4R_c/a) - 1. \tag{56}$$

APPENDIX II. STABILITY OF THE RING MODEL FOR THE ZERO-FIELD STATE OF THE SPHERE

From symmetry considerations the ring model is an equilibrium state. However, in order that this equilibrium be stable, the Hessian of the energy function with respect to any set of chosen functions describing a perturbation from this state must be positive.

Let the sphere be defined in a cylindrical coordinate system (r,φ,z) and let ϵ be the angle between the magnetization vector and the horizontal plane. In order to facilitate the calculation of the self-magnetostatic energy, ϵ is assumed to be independent of z. From symmetry considerations, ϵ is also assumed to be independent of φ. In order to study the stability of the state $\epsilon=0$, only angles $\epsilon \ll 1$ are considered.

The surface charge σ on the sphere is given by

$$\sigma = I_s \epsilon \cos\theta, \tag{57}$$

where θ is the polar angle. Let the angle ϵ be represented by the series

$$\epsilon = \sum_{n=1}^{\infty} B_{2n-1} P_{2n-1}/\cos\theta, \tag{58}$$

where B_{2n-1} are constants and P_{2n-1} are Legendre polynomials,[41] so that E_m can be readily calculated.

Only polynomials of odd order are taken in order to satisfy the symmetry relation

$$\sigma(\theta) = -\sigma(\pi-\theta).$$

Upon substituting from (58) into (57); the surface charge is

$$\sigma = I_s \sum_{n=1}^{\infty} B_{2n-1} P_{2n-1}, \tag{59}$$

and the associated energy E_m is

$$E_m = \sum_{n=1}^{\infty} B_{2n-1}^2 8\pi^2 I_s^2 R^3/(4n-1)^2, \tag{60}$$

and with the notation

$$R_0 = A^{\frac{1}{2}}/I_s \quad \text{and} \quad S = R/R_0,$$

one obtains

$$E_m = 4\pi A R \sum_{n=1}^{\infty} 2B_{2n-1}^2 (4n-1)^{-2} S^2. \tag{61}$$

The exchange energy derived from (7) is

$$E_x = 2A \int_{a/2}^{R}\int_{0}^{(R^2-r^2)^{\frac{1}{2}}} [(d\omega/dr)^2 + \sin^2\omega/r^2] 2\pi r dz dr. \tag{62}$$

Writing $x=[1-(r/R)^2]^{\frac{1}{2}}=\cos\theta$, and using

$$\omega = 90-\epsilon, \quad \epsilon \ll 1,$$

one finds, upon integrating with respect to z, that

$$E_x = 4\pi A R \int_{0}^{1-a^2/8R^2} [(1-x^2)(d\epsilon/dx)^2 - x^2\epsilon^2/(1-x^2)] dx. \tag{63}$$

Upon substituting (58) in (63), E_x can be calculated

[37] L. Néel, Compt. rend. **228**, 664 (1949).
[38] Sixtus, Kronenberg, and Tenzer, J. Appl. Phys. **27**, 1051 (1956).
[39] W. F. Brown, Revs. Modern Phys. **17**, 15 (1945).
[40] Rathenau, Smit, and Stuyts, Z. Physik **133**, 250 (1952).
[41] E. Jahnke and F. Emde, reference 24, p. 108.

and will be in the form of

$$E_x=\sum_{ij} E_x^{ij}B_iB_j. \tag{64}$$

In order that the state $\epsilon=0$ be a minimum energy state, the Hessian of the total energy

$$E=E_x+E_m$$

with respect to the coefficients B_{2n-1} should be positive.

The calculation yields for the Hessian

$$\frac{|\mathfrak{H}|}{8\pi AR}=\begin{vmatrix} 1-P+\frac{2\pi}{9}S^2 & \frac{11}{6}-P & \frac{137}{60}-P & \cdots \\ \frac{11}{6}-P & \frac{31}{6}-P+\frac{2\pi}{49}S^2 & -\frac{23}{60}-P & \cdots \\ \frac{137}{60}-P & -\frac{23}{60}-P & \frac{697}{60}-P+\frac{2\pi}{121}S^2 & \cdots \\ \cdots & \cdots & \cdots & \cdots \end{vmatrix}, \tag{65}$$

where

$$P=\ln(4R_0S/A).$$

The Hessian as given above is an infinite determinant. One is forced to study its behavior by studying the series formed by its principal minors.

In the first approximation,

$$|\mathfrak{H}|_1=8\pi AR[1-\ln(4R_0S/A)+(2\pi/9)S^2], \tag{66}$$

which is associated with

$$x\epsilon=B_1P_1.$$

$|\mathfrak{H}|_1$ is positive down to the critical size S_{c1}, becoming negative below it. S_{c1} is identical with the critical size as usually calculated.[8] For iron, $R_{c1}\approx 110$ A.

This might indicate that for particles larger than R_{c1} the ring model is of stable equilibrium. However, examining the second and third approximations to the Hessian which are associated with $x\epsilon=B_1P_1+B_3P_3$ and $x\epsilon=B_1P_1+B_3P_3+B_5P_5$, respectively, one finds that the critical radius increases to 220 A and 350 A respectively, hinting that taking more terms will push the critical radius always higher. This suggest that the ring model is never of stable equilibrium.

A second approach to this problem is to assume for the perturbation

$$\begin{aligned} &\epsilon=k(b-r) && \text{for} \quad r\leqslant b, \\ &\epsilon=0 && \text{for} \quad r\geqslant b, \end{aligned} \tag{67}$$

where b is a constant and k is calculated to minimize the energy. The variable part of E_x is

$$\begin{aligned} E_x&=8\pi AR\int_{a/2}^{b}[(d\epsilon/dr)^2-\epsilon^2/r^2]rdr, \\ E_x&=8\pi ARk^2b^2[2-a/b-\ln(2b/a)]. \end{aligned} \tag{68}$$

The variable part of the magnetostatic energy is

$$E_m<\tfrac{1}{2}N(kbI_s)^2\pi b^2 2R, \tag{69}$$

as the right-hand side is the energy of the region where $\epsilon\neq 0$ taken as that of an ellipsoid. Here $b\ll R$ is assumed. In this case, N is given by

$$N=4\pi b^2R^{-2}\ln(2R/b). \tag{70}$$

The total energy E is

$$E<k^2 8\pi ARb^2[2-a/b-\ln(2b/a) +\tfrac{1}{2}\pi b^4R^{-2}R_0^{-2}\ln(2R/b)]. \tag{71}$$

The condition for stability here is

$$\partial^2E/\partial k^2>0. \tag{72}$$

Taking for iron $a\approx 3$ A, $R_0\approx 60$ A, and choosing $b=30$ A, one finds that

$$\partial^2E/\partial k^2\approx 16\pi ARb^2(-1+1,6x^{-2}\ln x). \tag{73}$$

Here $x=2R/b$. Equation (73) shows that $\epsilon=0$ is never stable as $\partial^2E/\partial k^2<0$ for any value of x.

APPENDIX III. THE HOLLOW CYLINDER

In Eq. (15) it is found that the angle ω varies with the radius according to the relation

$$\omega=BJ_1[(-h\pi)^{\frac{1}{2}}Sx]+CN_1[(-h\pi)^{\frac{1}{2}}Sx], \tag{74}$$

with the boundary conditions

$$d\omega/dx=0 \quad \text{at} \quad x=1 \quad \text{and} \quad x=\alpha. \tag{75}$$

Here α is the reduced inner radius.

When one uses (35), the two boundary conditions yield the equations

$$B[J_0(\mu)-J_1(\mu)/\mu]+C[N_0(\mu)-N_1(\mu)/\mu]=0, \tag{76}$$

$$B[J_0(\mu\alpha)-J_1(\mu\alpha)/\mu\alpha] +C[N_0(\mu\alpha)-N_1(\mu\alpha)/\mu\alpha]=0, \tag{77}$$

where

$$\mu=(-h\pi)^{\frac{1}{2}}S. \tag{78}$$

The solutions

$$B=0, \quad C=0 \tag{79}$$

hold before nucleation. At nucleation

$$B\neq 0, \quad C\neq 0, \tag{80}$$

so that the determinant of the coefficients of B and C must vanish, yielding

$$\frac{J_0(\mu)-J_1(\mu)/\mu}{J_0(\mu\alpha)-J_1(\mu\alpha)/\mu\alpha}=\frac{N_0(\mu)-N_1(\mu)/\mu}{N_0(\mu\alpha)-N_1(\mu\alpha)/\mu\alpha}. \tag{81}$$

This equation gives $\mu=\mu(\alpha)$, and with (78) the nucleation field h_n is found as a function of the inner radius α.

From (81), one finds that, for $\alpha\ll 1$,

$$h_n=h_0(1-4.2\alpha^2), \tag{82}$$

where h_0 is the nucleation field as given in (19). Following Néel,[8] the value of the inner radius is taken to equal half a lattice constant. One has then

$$h_n\approx h_0[1-(a/R)^2], \tag{83}$$

and as one considers only $R>R_0$ (Fig. 4) and $a/R_0\ll 1$, one sees that h_n is essentially the same if one assumes the boundary conditions $\omega=0$ at $x=0$ or if one allows for a mobile limit at $x=a/2R$.

APPENDIX IV. DISCONTINUITY OF MAGNETIZATION AT THE CURLING NUCLEATION IN THE CYLINDER

In Eq. (10), the total energy is found to be

$$E=\frac{2A}{R^2}\int_{a/2R}^{1}[x(d\omega/dx)^2+\sin^2\omega/x-2\pi S^2hx\cos\omega]dx \tag{84}$$

$$=\frac{2A}{R^2}\int_{a/2R}^{1}\{x(d\omega/dx)^2+\omega^2/x-2\pi S^2hx(1-\omega^2/2)$$
$$-2\pi S^2hx[\omega^4/4!-O(\omega^6)]$$
$$-[(2\omega)^4/4!-O(\omega^6)]/2x\}dx. \tag{85}$$

When one takes only terms up to ω^2, the nucleation function is [according to (15)]

$$\omega=BZ_1[(-h\pi)^{\frac{1}{2}}Sx], \tag{86}$$

where Z_1 is a linear combination of Bessel and Neumann functions.

At nucleation,

$$\int_{a/2R}^{1}[x(d\omega/dx)^2+\omega^2/x-2\pi S^2h_nx(1-\omega^2/2)]dx$$
$$=\text{constant}, \tag{87}$$

so that

$$E=\text{constant}-\frac{2A}{R^2}\int_{a/2R}^{1}\omega^4x^{-1}(\pi S^2h_nx^2/12+\tfrac{1}{3})dx. \tag{88}$$

For small values of ω,

$$E<\text{const}-\frac{2A}{R^2}\int_{a/2R}^{1}\omega^4x^{-1}(-3.39/12+\tfrac{1}{3})dx, \tag{89}$$

where $\pi S^2h_n=-3.39$ is taken from (19).

It is seen that E decreases with ω, thus assuring a discontinuous change of the magnetization at nucleation.

APPENDIX V. SELF-MAGNETOSTATIC ENERGY ASSOCIATED WITH THE BUCKLING CONFIGURATION

According to (23), the surface charge σ on the cylinder is given by

$$\sigma=\sum_{m=1}^{\infty}\sigma_{2m-1}=I_s\cos\varphi\sum_{m=1}^{\infty}\omega_{2m-1}\cos\left[(2m-1)\frac{\pi}{T}z\right]. \tag{90}$$

The corresponding solution of the Laplace equation for the magnetostatic potential F yields

$$F=\sum_{m=1}^{\infty}A_{2m-1}J_1\left[i(2m-1)\frac{\pi}{T}r\right]$$
$$\times\cos\varphi\cos\left[(2m-1)\frac{\pi}{T}z\right] \tag{91}$$

for $r\leqslant R$, and

$$F=\sum_{m=1}^{\infty}B_{2m-1}H_1^{(1)}\left[i(2m-1)\frac{\pi}{T}r\right]$$
$$\times\cos\varphi\cos\left[(2m-1)\frac{\pi}{T}z\right] \tag{92}$$

for $r\geqslant R$. Here A_{2m-1} and B_{2m-1} are constants.

Equating the potential at $r=R$ yields

$$B_{2m-1}=A_{2m-1}J_1\left[i(2m-1)\frac{\pi}{T}R\right]\Big/$$
$$H_1^{(1)}\left[i(2m-1)\frac{\pi}{T}R\right]. \tag{93}$$

The divergence of H equals $4\pi\sigma$, and is found by using $H=\text{grad}F$ and (91), (92) so that

$$A_{2m-1}\frac{d}{dr}J_1\left[i(2m-1)\frac{\pi}{T}r\right]$$
$$-B_{2m-1}\frac{d}{dr}H_1^{(1)}\left[i(2m-1)\frac{\pi}{T}r\right]=4\pi I_s\omega_{2m-1} \tag{94}$$

at $r=R$.

From (93) and (94), one finds that

$$A_{2m-1}=2\pi^2\omega_{2m-1}iRI_sH_1^{(1)}\left[i(2m-1)\frac{\pi}{T}R\right]. \tag{95}$$

The energy per unit volume of the cylinder is

$$\bar{E}=\pi R^2 8\pi(16\pi^2R^2T)^{-1}\int_0^{2T}\int_0^{2\pi}4\pi F\sigma R d\varphi dz. \quad (96)$$

Using this and (90), (91), and (95), one obtains after integration

$$\bar{E}=\sum_{m=1}^{\infty}\tfrac{1}{2}\pi^2 I_s^2\omega_{2m-1}{}^2 iH_1{}^{(1)}\left[i(2m-1)\frac{\pi}{T}R\right]\times J_1\left[i(2m-1)\frac{\pi}{T}R\right]. \quad (97)$$

PHYSICAL REVIEW VOLUME 106, NUMBER 3 MAY 1, 1957

Surface States on Silicon and Germanium Surfaces*

H. STATZ, G. DEMARS, L. DAVIS, JR., AND A. ADAMS, JR.
Research Division, Raytheon Manufacturing Company, Waltham, Massachusetts
(Received December 26, 1956)

Interface states are found in the upper half of the energy gap of silicon and germanium. On weakly oxidized surfaces, they lie 0.42 and 0.13 ev above the intrinsic position of the gap with approximate densities 10^{11} to 10^{12} and 10^{10} to 10^{11} for silicon and germanium, respectively. On well-oxidized surfaces, interface states are found approximately 0.44 to 0.48 ev and 0.18 ev above the intrinsic position of the gap with densities of around 10^{12} and 10^{11} to 10^{12} for silicon and germanium, respectively. At large bias voltages, high electric fields exist in the oxide film. Changes in the structure of the interface states in the upper half of the gap of silicon are found. A model is given which can account for the experimental observation.

INTRODUCTION

In a previous paper,[1] measurements of inversion layers on *n*-type germanium and silicon have been reported. This paper represents an extension of reference 1 to measurements of inversion layers on *p*-type germanium and silicon. Essentially, the same notation and terminology will be used. From the steady state and nonsteady state measurements, it has been deduced previously that on both germanium and silicon there is a very high density of surface states on or near the surface of the oxide film (outer surface states) and a much smaller density at the interface of the semiconductor and the semiconductor oxide film (interface states). The outer surface states appear to result from adsorbed atoms of the surrounding ambient gas. The measurements of the interface states have been interpreted in terms of one localized state 0.138 ev and 0.455 ev below the middle of the gap for germanium and silicon, respectively. The densities were approximately 10^{11} states/cm^2 for germanium and 10^{12} states/cm^2 for silicon.

In the meantime, other contributions from workers in the field have appeared in the literature which deal directly or indirectly with a determination of the interface states.[2–8] The work of Bardeen *et al.*[3] essentially confirmed the previous finding for interface states in the lower half of the gap of germanium. It appears, however, that in addition to these localized states there is a continuous distribution of surface states near the middle of the forbidden gap. The total number of these distributed states is considerably smaller than that of the localized ones.[3] Measurements of interface states by conduction measurements of inversion layers are difficult and sometimes even impossible for states lying close to the center of the forbidden gap. In such measurements, the charge in the interface states as a function of the quasi-Fermi level for holes or electrons is deduced from "pulsed" conductance measurements as a function of bias voltage. If the quasi-Fermi level describing the distribution of the majority carriers in the surface layer is close to the middle of the gap, then the conductance of the inversion layer is very small. The saturation current flowing across the junction between the inversion layer and the bulk of the material gives rise to an ohmic drop in the inversion layer so that the bias voltage between the bulk of the semiconductor and the inversion layer is not constant along the base region of the *n-p-n* and *p-n-p* type semiconductor bars. The inversion layer technique is, therefore, not easily applicable for states near the middle of the band gap. In addition, as will be shown, the occupancy of the interface states may not be described by the quasi-Fermi level for majority carriers if the ratio of the capture cross for electrons and holes is unfavorable.

* Supported in part by the Bureau of Ships.
[1] Statz, deMars, Davis, and Adams, Phys. Rev. **101**, 1272 (1956).
[2] W. L. Brown, Phys. Rev. **100**, 590 (1955).
[3] Bardeen, Coovert, Morrison, Schrieffer, and Sun, Phys. Rev. **104**, 47 (1956).
[4] W. H. Brattain and C. G. B. Garrett, Bell System Tech. J. **35**, 1019 (1956).
[5] C. G. B. Garrett and W. H. Brattain, Bell System Tech. J. **35**, 1041 (1956).
[6] Many, Margoninski, Harnik, and Alexander, Phys. Rev. **101**, 1433 (1956).
[7] Harnik, Many, Margoninski, and Alexander, Phys. Rev. **101**, 1434 (1956). [See also contribution by Many, Harnik, and Margoninski to appear in *Proceedings of the Conference on the Physics of Semiconductor Surfaces, University of Pennsylvania, Philadelphia, Pennsylvania, June, 1956* (to be published)].
[8] H. C. Montgomery and W. L. Brown, Phys. Rev. **103**, 865 (1956).